

# Buckling of axially compressed thin cylindrical shells with functionally graded middle layer

Shi-Rong Li<sup>a,\*</sup>, R.C. Batra<sup>b</sup>

<sup>a</sup>*Department of Engineering Mechanics, Lanzhou University of Technology, Lanzhou 730050, PR China*

<sup>b</sup>*Department of Engineering Science and Mechanics, Virginia Polytechnic Institute and State University, Blacksburg, VA 24061, USA*

Received 1 March 2006; received in revised form 25 August 2006; accepted 18 October 2006

Available online 19 December 2006

## Abstract

Buckling of a simply supported three-layer circular cylindrical shell under axial compressive load is studied. The inner and outer layers of the shell are comprised of the same homogeneous and isotropic material, and the middle layer is made of an isotropic functionally graded (FG) material whose Young's modulus varies either affinely or parabolically in the thickness direction from its value for the material of the inner layer to that of the outer layer. The solution is expressed in terms of trigonometric functions that identically satisfy displacement type boundary conditions at the edges. Buckling loads for different values of the geometric parameters and the variation in material parameters of the middle layer are computed. Numerical results show that buckling modes are symmetric in the circumferential coordinate, and the buckling load decreases with an increase in the radius to thickness ratio, and increases with an increase in the average value of Young's modulus of the middle layer. The increase in the length to radius ratio has no effect on the buckling load, and it increases the axial wave number of the buckled shapes.

© 2006 Elsevier Ltd. All rights reserved.

*Keywords:* Functionally graded materials; Thin cylindrical shell; Buckling load

## 1. Introduction

Circular cylindrical shells are widely used in many engineering fields such as aerospace, chemical, civil, mechanical, naval, and nuclear. A predominant mode of failure of axially compressed thin cylindrical shells is axial buckling, and the problem has been studied for more than a century [1–12]. von Karman and Tsien [4] have derived an expression for the buckling load and have also analyzed the post-buckling equilibrium path of an axially compressed thin homogeneous cylindrical shell. They showed that during the post-buckled stage, the load sustained by the shell drops with an increase in its deflection. Winterstetter and Schmidt [5] have conducted a comprehensive experimental and numerical investigation of the buckling of a steel cylindrical shell under combined loading. Kim and Kim [6] used the commercial finite element code ABAQUS to analyze the effect of geometric

imperfections on the buckling of axially compressed cylindrical shells and tanks. Pinna and Ronalds [7] have studied numerically the buckling and post-buckling of cylindrical shells with one end pinned and the other free, and computed the collapse and bifurcation loads. Eslami [9,10] employed the Wan-Donnell and Koiter shell theories to investigate buckling deformations of isotropic and orthotropic laminated cylindrical shells subjected to mechanical and thermal loads. Shen [11,12] used the perturbation method to analyze the thermal post-buckling of axially loaded and pressure-loaded cylindrical shells made of functionally graded (FG) materials.

Weaver [13] has pointed out that an axially compressed cylindrical shell can fail either by global buckling with a wavelength related to its length, or by local buckling with a wavelength related to the shell thickness, or by the yielding of the material of the shell. Furthermore, the axial buckling loads of thin-walled cylindrical shells are highly sensitive to nonuniformities in the wall thickness [14,15].

The motivation for the present work is provided by our interest in analyzing buckling of multi-walled carbon

\*Corresponding author.

*E-mail addresses:* [lizr@lut.cn](mailto:lizr@lut.cn) (S.-R. Li), [rbatra@vt.edu](mailto:rbatra@vt.edu) (R.C. Batra).

nanotubes (CNT) where van der Waals forces among atoms on two adjacent walls of the tube tend to resist buckling of the tubes. These forces act normal to the walls and depend upon the distance between them. While studying the buckling of a double-walled CNT Ru [8] simulated van der Waals forces by presuming that a pressure acts on the outer surface of the inner wall and the inner surface of the outer wall and its magnitude is inversely proportional to the distance between the two walls. Each wall of the CNT was replaced by a cylindrical tube comprised of an isotropic homogeneous and linear elastic material. Ru [8] used the classical shell theory to study buckling of a simply supported double-walled CNT under axial loads. Sears and Batra [16] also replaced each CNT by an equivalent continuum cylindrical tube, derived an expression for the van der Waals force, explored different methods of simulating van der Waals forces and used molecular mechanics simulations, Euler’s buckling theory, and the finite element method to study buckling of a double-walled CNT. They found that a multi-walled tube (MWNT) of large aspect ratio (length/diameter) and clamped at the top and the bottom surfaces buckles as a column with the axial strain at buckling given reasonably well by the Euler buckling theory applied to the equivalent continuum structure. However, a MWNT of low-aspect ratio buckled in shell wall buckling mode with the axial strain at buckling equaling that of one of its constituent single-walled CNTs.

Here, we use Flügge’s shell theory to study deformations of a simply supported thin circular cylindrical shell with the inner and the outer layers made of a homogenous and isotropic linear elastic material and the middle layer comprised of an inhomogeneous isotropic Hookean material with Young’s modulus varying continuously in the thickness direction from that of the material of the inner layer to that of the material of the outer layer. Poisson’s ratio of the material of the middle layer is taken to be constant. By assuming the solution of equilibrium equations in the form of trigonometric series that exactly satisfy the boundary conditions, an algebraic equation is derived for the axial buckling load of the shell. The effect of various material and geometric parameters on the axial buckling load is computed. Because of the assumption of the shell being thin, the analysis applies to a MWNT only when its thickness/radius is very small and length/radius very large.

**2. Formulation of the problem**

*2.1. Governing equations*

We consider a simply supported three-layered circular cylindrical shell of length  $l$ , wall thickness  $h$ , and undeformed mid-surface radius  $R$  as shown in Fig. 1. Assume that materials of the inner and the outer layers is isotropic, homogeneous, and Hookean, and that of the middle layer is isotropic, inhomogeneous and Hookean

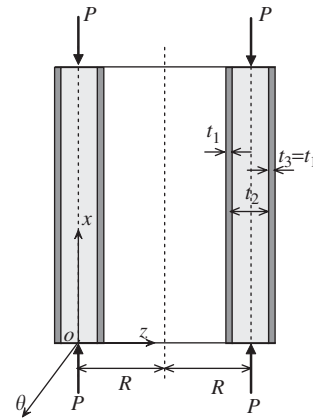


Fig. 1. Schematic sketch of the problem studied, and the location of coordinate axes.

with Young’s modulus varying continuously in the thickness direction from Young’s modulus of the material of the inner layer to that of the material of the outer layer. Thus, Young’s modulus is continuous across interfaces between the middle layer and the inner and the outer layers. Thicknesses of the inner, middle and outer layers are  $t_1$ ,  $t_2$  and  $t_3$ , respectively, and  $h = t_1 + t_2 + t_3$ . For  $t_1 = t_3 = 0$ , the shell is made of a FG material, and for  $t_2 = 0$ , it is made of a homogeneous material.

As shown in Fig. 1, we use cylindrical coordinates with the origin located at the mid-surface of the cylinder, and coordinates  $x$ ,  $\theta$  and  $z$  in the axial, the circumferential and the thickness directions, respectively. The top and the bottom surfaces of the cylinder are subjected to a uniformly distributed axial compressive load  $P$ . We use the classical shell theory [1–3] and hence the following kinematic relations:

$$U = u - \frac{zw'}{R}, \quad V = \frac{(R+z)v}{R} - \frac{zw^\bullet}{R}, \quad W = w, \quad (1)$$

where  $u(x,\theta)$ ,  $v(x,\theta)$  and  $w(x,\theta)$  are, respectively, the axial, the circumferential and the radial displacements of a point on the mid-surface,  $U$ ,  $V$  and  $W$  are the corresponding displacements of a point  $(x,\theta,z)$  of the shell,  $(\cdot)' = R\partial/\partial x$ , and  $(\cdot)^\bullet = \partial/\partial\theta$ . Here we have tacitly assumed that the displacement  $W$  does not depend upon  $z$ .

The normal and the shear strains at a point of the shell are given by [2]

$$\varepsilon_x = \frac{U'}{R}, \quad \varepsilon_\theta = \frac{V^\bullet + W}{R+z}, \quad \gamma_{x\theta} = \frac{V'}{R} + \frac{U^\bullet}{R+z}. \quad (2)$$

Substitution from Eq. (1) into Eq. (2) yields

$$\varepsilon_x = \frac{u'}{R} - \frac{z}{R^2}w'', \quad (3a)$$

$$\varepsilon_\theta = \frac{v^\bullet}{R} - \frac{z}{R} \frac{w^\bullet^\bullet}{R+z} + \frac{w}{R+z}, \quad (3b)$$

$$\gamma_{x\theta} = \frac{u^{\bullet}}{R+z} + \frac{R+z}{R^2} v' - \left( \frac{z}{R} + \frac{z}{R+z} \right) \frac{w^{\bullet}}{R}. \quad (3c)$$

2.2. Constitutive equations

For an isotropic linear elastic material, we have the following constitutive relations:

$$\sigma_x = \frac{E}{1-\nu^2} (\epsilon_x + \nu\epsilon_\theta), \quad (4a)$$

$$\sigma_\theta = \frac{E}{1-\nu^2} (\epsilon_\theta + \nu\epsilon_x), \quad (4b)$$

$$\tau_{x\theta} = \frac{E}{2(1+\nu)} \gamma_{x\theta}, \quad (4c)$$

where  $\sigma_x$ ,  $\sigma_\theta$  and  $\tau_{x\theta}$  are, respectively, the axial, circumferential and shear stresses in the  $x-\theta$  plane;  $E$  is Young's modulus, and  $\nu$  the Poisson ratio, with equal constants  $E_1$  and  $\nu_1$  for the inner and the outer layers. For the middle layer, we assume that Poisson's ratio is a constant, and either

$$E_2(z) = E_1(k + 2(1-k)|z|/t_2), \quad -t_2/2 < z < t_2/2 \quad (5)$$

or

$$E_2(z) = E_1(k + 4(1-k)(z/t_2)^2), \quad -t_2/2 < z < t_2/2, \quad (6)$$

where  $k = E_0/E_1$ ,  $E_0 = E_2(0)$ . Functions (5) and (6) are plotted in Fig. 2.

2.3. Equilibrium equations and boundary conditions

Forces and moments at a point on the mid-surface of the shell are related to stresses within the shell as follows:

$$(N_x, N_{x\theta}) = \int_{-h/2}^{h/2} (\sigma_x, \tau_{x\theta})(1+z/R) dz, \quad (7a)$$

$$(M_x, M_{x\theta}) = \int_{-h/2}^{h/2} (z\sigma_x, z\tau_{x\theta})(1+z/R) dz, \quad (7b)$$

$$(N_\theta, N_{\theta x}) = \int_{-h/2}^{h/2} (\sigma_\theta, \tau_{\theta x}) dz, \quad (7c)$$

$$(M_\theta, M_{\theta x}) = \int_{-h/2}^{h/2} (z\sigma_\theta, z\tau_{\theta x}) dz. \quad (7d)$$

Substitution from Eqs. (3) and (4) into Eq. (7) yields

$$\begin{pmatrix} \{N\} \\ \{M\} \end{pmatrix} = \begin{bmatrix} [A] & [B] \\ [C] & [D] \end{bmatrix} \begin{pmatrix} \{d_m\} \\ \{d_t\} \end{pmatrix}, \quad (8)$$

where

$$\{N\} = \{N_x, N_\theta, N_{x\theta}, N_{\theta x}\}^T, \quad \{M\} = \{M_x, M_\theta, M_{x\theta}, M_{\theta x}\}^T,$$

$$\{d_m\} = \{u', v^{\bullet}, u^{\bullet}, v'\}^T, \quad \{d_t\} = \{w'', w^{\bullet\bullet}, w^{\bullet}, w\}^T,$$

$\{N\}$  is the vector of membrane forces, and  $\{M\}$  the vector of resultant moments. The vector  $\{d_m\}$  is related to deformations of a point on the mid-surface,  $\{d_t\}$  the vector of the transverse deformations of the shell,  $[A]$  the extensional rigidity matrix,  $[B]$  and  $[C]$  the bending–stretching and the stretching–bending coupling rigidity matrices, respectively, and  $[D]$  is the matrix of bending rigidity. Definitions of components of these matrices and analytical expressions of their non-zero elements that involve material and geometric parameters are given in Appendix A.

Equations governing static deformations of a cylindrical shell (e.g., see [2]) are:

$$RN'_x + RN_{\theta x} - Pu'' = 0, \quad (10)$$

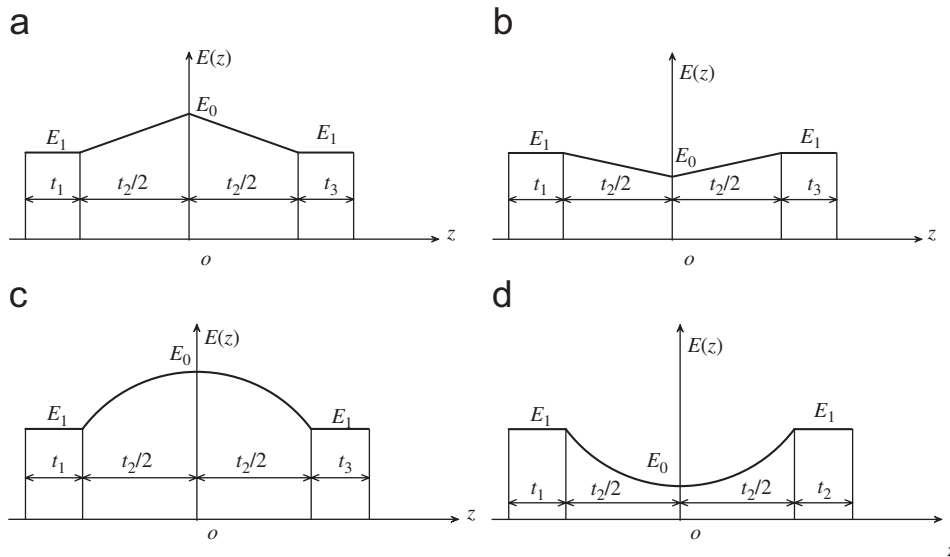


Fig. 2. Variation in the thickness direction of Young's modulus,  $E$ , of the middle layer: (a) affine variation,  $k > 1$ ; (b) affine variation,  $k < 1$ ; (c) parabolic variation,  $k > 1$ ; (d) parabolic variation,  $k < 1$ .

$$RN_{\theta}^{\bullet} + RN'_{x\theta} + M_{\theta}^{\bullet} + M'_{x\theta} - Pv'' = 0, \quad (11)$$

$$M''_x + M'_{x\theta} + M'_{\theta x} + M_{\theta}^{\bullet\bullet} - RN_{\theta} - Pw'' = 0. \quad (12)$$

Substitution from Eq. (8) into Eqs. (10)–(12) gives the following three partial differential equations for the determination of the mid-surface displacements  $u$ ,  $v$  and  $w$ :

$$A_{11}u'' + A_{43}u^{\bullet\bullet} + A_{12}^*v^{\bullet} + B_{11}w''' + B_{12}^*w'^{\bullet\bullet} + B_{14}w' - Pu''/R = 0, \quad (13)$$

$$A_{34}^*v'' + A_{22}^*v^{\bullet\bullet} + A_{21}^*u^{\bullet} + B_{22}^*w^{\bullet\bullet\bullet} + B_{21}^*w''^{\bullet} + B_{24}^*w^{\bullet} - Pv''/R = 0, \quad (14)$$

$$D_{11}w'''' + D_{12}^*w''^{\bullet\bullet} + D_{22}w^{\bullet\bullet\bullet\bullet} + (D_{14}^* - P)w'' + D_{24}^*w^{\bullet\bullet} - RB_{24}w + C_{11}u''' + C_{21}^*u^{\bullet\bullet} + C_{12}^*v''^{\bullet} + C_{22}v^{\bullet\bullet\bullet} - RA_{21}u' - RA_{22}v^{\bullet} = 0. \quad (15)$$

Expressions for parameters with the superscript star are given in Appendix B.

Boundary conditions for simply supported end surfaces of the cylindrical shell are:

$$A_{11}u' + A_{12}v^{\bullet} + B_{11}w'' + B_{12}w^{\bullet\bullet} = 0 \quad \text{at } x = 0, l, \quad (16)$$

$$C_{11}u' + C_{12}v^{\bullet} + D_{11}w'' + D_{12}w^{\bullet\bullet} = 0 \quad \text{at } x = 0, l. \quad (17)$$

### 3. Solution for bucking modes and loads

In view of boundary conditions (16) and (17), we consider solutions of Eqs. (13)–(15) of the form

$$\begin{aligned} u &= X_1 \cos(m\theta) \cos(\lambda_n x/R), \\ v &= X_2 \sin(m\theta) \sin(\lambda_n x/R), \\ w &= X_3 \cos(m\theta) \sin(\lambda_n x/R), \end{aligned} \quad (18)$$

that identically satisfy the boundary conditions for  $\lambda_n = n\pi R/l$  with  $m$  and  $n$  being integers. In Eq. (18) unknown constants  $X_i$  ( $i = 1, 2, 3$ ) represent amplitudes of a buckled mode shape. We substitute from Eq. (18) into equilibrium Eqs. (13)–(15), note that the trigonometric functions drop out, and arrive at the following algebraic equations:

$$(a_{11} - p)X_1 + a_{12}X_2 + a_{13}X_3 = 0, \quad (19)$$

$$a_{21}X_1 + (a_{22} - p)X_2 + a_{23}X_3 = 0, \quad (20)$$

$$a_{31}X_1 + a_{32}X_2 + (a_{33} - p)X_3 = 0, \quad (21)$$

where  $p = P/C$  with  $C = E_1 h / (1 - \nu_1^2)$  is a non-dimensional load parameter, and  $a_{ij}$  ( $i, j = 1, 2, 3$ ) are dimensionless coefficients associated with the shell geometry and its material parameters. Henceforth, we assume that the inner and the outer layers have the same thickness, i.e.,  $t_1 = t_3$ , and have listed in Appendix C analytical expressions for  $a_{ij}$ .

The necessary and sufficient condition for the system of homogeneous Eqs. (19)–(21) to have a non-trivial solution for the amplitude  $X_i$  is that the determinant of the matrix of their coefficients must vanish. That is

$$\begin{vmatrix} a_{11} - p & a_{12} & a_{13} \\ a_{21} & a_{22} - p & a_{23} \\ a_{31} & a_{32} & a_{33} - p \end{vmatrix} = 0. \quad (22)$$

The minimum root of Eq. (22) equals the non-dimensional buckling load  $p$ , and the corresponding buckling mode can then be computed from any two of the three Eqs. (19)–(21).

## 4. Numerical results

We use Newton's iteration method to find a root of Eq. (22). From expressions of coefficients  $a_{ij}$  given in Appendix C, we deduce that the root of Eq. (22) depends not only on the shell geometry and material parameters but also on wave numbers  $m$  and  $n$  that give the deformed shape of the shell in the circumferential and the axial directions, respectively. The pair  $m$  and  $n$  corresponding to the smallest root of Eq. (22) is determined by an iterative method.

### 4.1. Verification of the numerical scheme

We first consider a circular cylindrical shell made of a homogeneous material (i.e.,  $k = 1$ ). The non-dimensional buckling stress,  $\sigma_{cr}/E$ , as a function of the geometrical parameter,  $\delta = R/h$ , radius-to-thickness ratio, is given by [1–4,6]

$$\frac{\sigma_{cr}}{E} = \frac{1}{\delta \sqrt{3(1 - \nu^2)}}. \quad (23)$$

The non-dimensional axial buckling stresses for different values of  $\delta$  and length/radius as computed from Eq. (22) with  $m = 0$  are compared with those obtained from Eq. (23) in Table 1. It is clear that for a given value of  $\delta$ , the computed axial buckling stress is independent of  $l/R$ , and it equals that derived from Eq. (23). Furthermore, the buckling mode is axially symmetric (i.e.,  $m = 0$ ), and the axial wave number,  $n$ , increases with an increase in  $\delta$  and  $l/R$ .

### 4.2. Results for a functionally graded cylinder

For  $m = 0, 1, 2, 3, 4$ , and 5, and  $E$  given by Eq. (5) or (6), Fig. 3(a) exhibits the variation of the minimum root of Eq. (22) with  $\lambda_n$ ; values of other parameters are listed in the caption of Fig. 3. It is evident that the minimum root of Eq. (22) decreases with an increase in  $\lambda_n$ , attains a minimum value and then increases. The minimum value  $9.38 \times 10^{-4}$  of  $p$  occurs for  $\lambda_n = 37.3$ , and is essentially

Table 1

Non-dimensional axial buckling stress  $(\sigma_{cr}/E) \times 10^4$  of a homogeneous cylindrical shell deformed in an axially symmetric mode ( $m = 0, \nu = 0.3$ )

$\delta$	$l/R$						Eq. (23)
	0.5	1.0	2.0	3.0	4.0	5.0	
200	30.274(4*)	30.274(8)	30.274(16)	30.264(25)	30.248(33)	30.244(41)	30.261
400	15.166(6)	15.166(12)	15.127(23)	15.128(35)	15.127(46)	15.126(58)	15.130
600	10.088(7)	10.088(14)	10.088(28)	10.088(43)	10.086(57)	10.085(71)	10.087
800	7.5720(8)	7.5720(16)	7.5652(33)	7.5643(49)	7.5650(65)	7.5643(82)	7.5653
1000	6.0548(9)	6.0548(18)	6.0530(37)	6.0516(55)	6.0516(73)	6.0519(91)	6.0523

\*Numbers in brackets are the axial wave numbers of the buckling modes; the same notation is used in the following tables.

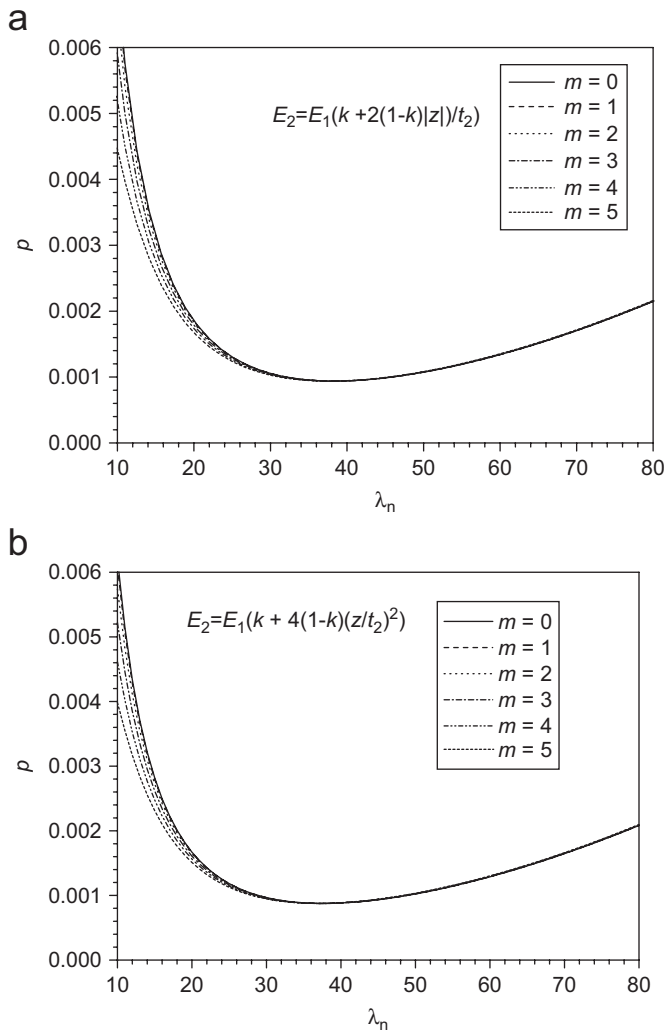


Fig. 3. The root  $p$  of Eq. (22) as a function of  $\lambda_n$  for a given circumferential wave number  $m$  ( $\delta = 500, \beta = 0.6, k = 0.2, l/R = 2.0$ ) with Young's modulus of the middle layer given by (a) Eq. (5), and (b) Eq. (6).

independent of the circumferential wave number  $m$  implying thereby that the axial buckling load can be computed by setting  $m = 0$  in Eq. (22). Results plotted in Fig. 3(b) for  $E$  given by Eq. (6) show the same

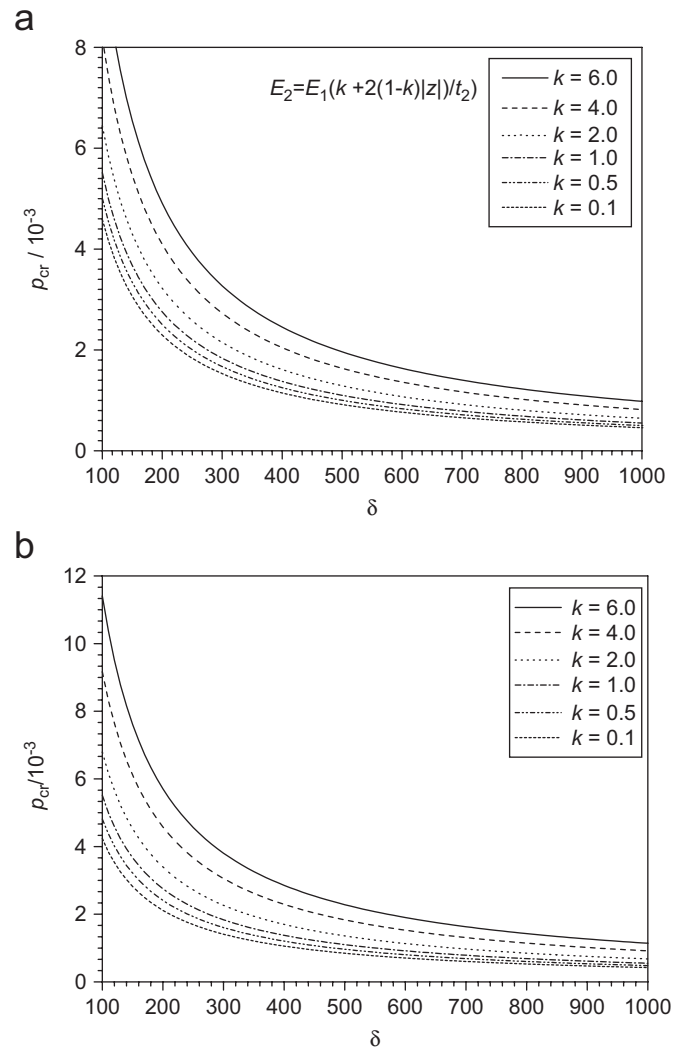


Fig. 4. Non-dimensional axial buckling load,  $p_{cr}/10^{-3}$ , versus the radius-to-thickness ratio,  $\delta$ , of the cylindrical shell for specified values of  $k$  ( $l/R = 2.0, \beta = 0.6, \nu_1 = \nu_2 = 0.3$ ) with Young's modulus of the middle layer given by (a) Eq. (5), and (b) Eq. (6).

characteristics as those in Fig. 3(a) for  $E$  given by Eq. (5). For  $k = 0.2$  in Eqs. (5) and (6), the affine variation in  $E$  for the middle layer results in a higher axial buckling load than the parabolic variation.

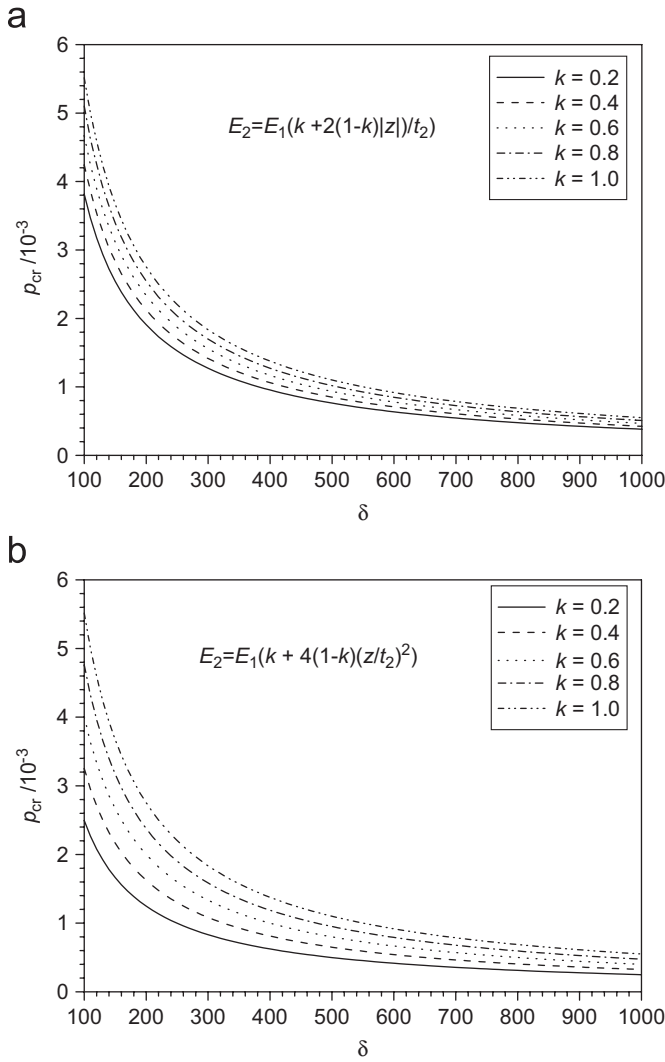


Fig. 5. Non-dimensional axial buckling load,  $p_{cr}/10^{-3}$ , versus the radius-to-thickness ratio,  $\delta$ , for the fully FG cylindrical shell for some specified values of  $k$  ( $l/R = 2.0$ ,  $\beta = 0.1$ ,  $\nu_1 = \nu_2 = 0.3$ ) with Young's modulus given by (a) Eq. (5), and (b) Eq. (6).

For  $\beta = t_1/t_2 = 0.6$  and different values of  $k$ , the variation with the parameter  $\delta$  of the non-dimensional axial buckling load,  $p_{cr}$ , is plotted in Fig. 4 by considering both the affine and the parabolic variations in Young's modulus of the middle layer. These results show that for a fixed value of  $\delta$ , the buckling load increases with an increase in  $k$ . For  $k < 1$ , the stiffness of the middle layer is less than that of the inner and the outer layers. Note that the bending rigidity of the middle layer increases with an increase in the value of  $k$ . Furthermore, for the same value of  $k$ , the buckling load for the shell with the affinely graded middle layer is greater than that of the shell with the parabolically graded middle layer. For  $t_2 = h$ , or  $\beta = 1$ , one gets a fully FG shell. The variation of  $p_{cr}$  with  $\delta$  is plotted in Fig. 5 for several values of  $k$ , and conclusions similar to those for results in Fig. 4 can be derived from them.

For Young's modulus of the middle layer given by Eq. (5), values of the axial critical buckling load of the cylindrical shell for different values of parameters  $k$  and  $l/R$  are listed in Table 2. It is observed that the buckling load increases with an increase in the value of  $k$  or equivalently with an increase in the overall stiffness of the middle layer, but is essentially independent of  $l/R$ . However, the axial wave number  $n$  increases with an increase in the length/radius in order to keep the value of  $\lambda_n$  constant for a definite buckling mode.

For Young's modulus given by Eq. (6) we have listed in Table 3 the non-dimensional axial buckling load for different values of  $\delta$  and  $k$ . It is evident that parameters  $\delta$  and  $k$  noticeably affect the buckling load  $p_{cr}$ ; the wave number of the buckled mode increases monotonically with an increase in  $\delta$ . However, for a fixed value of  $\delta$  the wave number is essentially independent of  $k$ . We note that  $\delta = 10$  is probably the lower limit for the shell to be classified as thin. Also, negligible differences

Table 2

The axial buckling load ( $p_{cr} \times 10^4$ ) for different values of  $k$  and  $l/R$  ( $m = 0$ ,  $\beta = 0.6$ ,  $\nu_1 = \nu_2 = 0.3$ ,  $\delta = 500$ , Young's modulus of the middle layer given by Eq. (5))

$k$	$l/R$						
	0.5	1.0	2.0	3.0	4.0	5.0	6.0
0.2	9.3965(6)	9.3965(12)	9.3965(24)	9.3923(37)	9.3907(49)	9.3906(61)	9.3909(73)
0.4	9.8318(6)	9.8318(12)	9.8101(25)	9.8100(37)	9.8101(50)	9.8092(62)	9.8100(74)
0.6	10.267(6)	10.238(13)	10.220(25)	10.219(38)	10.220(50)	10.218(63)	10.219(76)
0.8	10.702(6)	10.626(13)	10.626(26)	10.621(38)	10.619(51)	10.619(64)	10.620(77)
1.0	11.138(6)	11.013(13)	11.013(26)	11.013(39)	11.013(52)	11.013(65)	11.013(78)
1.2	11.502(7)	11.400(13)	11.400(26)	11.400(39)	11.400(52)	11.400(65)	11.400(79)
1.4	11.854(7)	11.788(13)	11.788(26)	11.781(40)	11.780(53)	11.780(66)	11.781(79)
1.6	12.205(7)	12.175(13)	12.157(27)	12.155(40)	12.157(54)	12.155(67)	12.155(80)
1.8	12.557(7)	12.557(14)	12.525(27)	12.529(41)	12.525(54)	12.526(68)	12.525(81)
2.0	12.909(7)	12.909(14)	12.894(27)	12.891(41)	12.893(55)	12.891(68)	12.891(82)

Table 3

The axial buckling load ( $p_{cr} \times 10^4$ ) for different values of  $\delta$  and  $k$  ( $m = 0$ ,  $\beta = 0.8$ ,  $l/R = 1.0$ ,  $\nu_1 = \nu_2 = 0.3$ , Young's modulus of the middle layer given by Eq. (5))

$\delta$	$k$					
	0.1	0.2	0.4	0.6	0.8	1.0
10	432.64(2)	445.99(2)	472.70(2)	499.40(2)	526.10(2)	552.79(2)
30	137.69(3)	142.83(3)	153.11(3)	163.39(3)	173.66(3)	183.94(3)
50	83.227(4)	86.202(4)	92.151(4)	98.101(4)	104.05(4)	110.00(4)
100	41.737(5)	43.474(5)	46.741(6)	49.546(6)	52.351(6)	55.156(6)
200	20.849(8)	21.594(8)	23.083(8)	24.5729(8)	26.061(8)	27.550(8)
300	13.828(9)	14.378(9)	15.438(10)	16.409(10)	17.380(10)	18.352(10)
400	10.377(11)	10.761(11)	11.530(11)	12.298(11)	13.067(11)	13.801(12)
500	8.2872(12)	8.6040(12)	9.2374(12)	9.8556(13)	10.434(13)	11.013(13)
600	6.9063(13)	7.1739(13)	7.7075(14)	8.1984(14)	8.6893(14)	9.1803(14)
700	5.9204(14)	6.1506(14)	6.5998(15)	7.0242(15)	7.4487(15)	7.8732(15)
800	5.1801(15)	5.3810(15)	5.7735(16)	6.1459(16)	6.5182(16)	6.8905(16)
900	4.6043(16)	4.7816(16)	5.1331(17)	5.4634(17)	5.7937(17)	6.1241(17)
1000	4.1444(17)	4.3024(17)	4.6185(17)	4.9182(18)	5.2140(18)	5.5099(18)

in the values of the buckling load for different values of  $m$  were found and these results are not included (e.g., see Fig. 3).

## 5. Conclusions

We have used Flügge's theory and a semi-inverse method to study the buckling of a thin cylindrical shell with FG middle layer surrounded by two homogeneous layers, and the material of each layer is assumed to be isotropic and Hookean. Young's modulus of the material of the middle layer is taken to vary either affinely or parabolically from that of the material of the inner layer to that of the material of the outer layer. The simply supported top and bottom surfaces of the shell are compressed axially by a load distributed uniformly on those surfaces. Displacements expressed in terms of trigonometric functions identically satisfy kinematic boundary conditions at the edge surfaces. These when substituted in the equilibrium equations yield an eigen value problem for the determination of the axial buckling load. It is found that a thin shell buckles in an axisymmetric mode. The dependence of the axial buckling mode upon various material and geometric parameters has been computed and presented either in Tables or as plots.

## Acknowledgements

Shi-Rong Li's work was supported in part by The National Natural Science Foundation of China Grant no. 10472039, and The Fund of Key Research Projects of the Lanzhou University of Technology. RCB's work was partially supported by the US Office of Naval Research Grant N00014-1-06-0567 with Dr. Y.D.S. Rajapakse as the program manager. Views expressed herein are those of authors and neither of funding agencies nor of authors' institutions.

## Appendix A

The rigidity matrices in Eq. (8) are

$$\begin{aligned}
 [A] &= \begin{bmatrix} A_{11} & A_{12} & 0 & 0 \\ A_{21} & A_{22} & 0 & 0 \\ 0 & 0 & A_{33} & A_{34} \\ 0 & 0 & A_{43} & A_{44} \end{bmatrix}, \\
 [B] &= \begin{bmatrix} B_{11} & B_{12} & 0 & 0 \\ B_{21} & B_{22} & 0 & 0 \\ 0 & 0 & B_{33} & B_{34} \\ 0 & 0 & B_{43} & B_{44} \end{bmatrix}, \\
 [C] &= \begin{bmatrix} C_{11} & C_{12} & 0 & 0 \\ C_{21} & C_{22} & 0 & 0 \\ 0 & 0 & C_{33} & C_{34} \\ 0 & 0 & C_{43} & C_{44} \end{bmatrix}, \\
 [D] &= \begin{bmatrix} D_{11} & D_{12} & 0 & 0 \\ D_{21} & D_{22} & 0 & 0 \\ 0 & 0 & D_{33} & D_{34} \\ 0 & 0 & D_{43} & D_{44} \end{bmatrix},
 \end{aligned}$$

and expressions for the non-vanishing elements of these matrices are given by

$$A_{11} = (R\zeta_0 + \xi_1)/R^2, \quad A_{12} = (R\eta_0 + \eta_1)/R^2,$$

$$A_{21} = \eta_0/R, \quad A_{22} = \xi_0/R,$$

$$A_{33} = \zeta_0/R, \quad A_{34} = (R^2\zeta_0 + 2R\zeta_1 + \zeta_2)/R^3,$$

$$A_{43} = \mu_2, \quad A_{44} = (R\zeta_0 + \zeta_1)/R^2,$$

$$\begin{aligned}
 B_{11} &= -(R\zeta_1 + \zeta_2)/R^3, \quad B_{12} = -\eta_1/R^2, \\
 B_{14} &= \eta_0/R, \quad B_{21} = -\eta_1/R^2, \\
 B_{22} &= -(\zeta_0 - R\mu_1)/R, \quad B_{24} = \mu_1, \\
 B_{33} &= -(2R\zeta_1 + \zeta_2)/R^3, \quad B_{43} = -(R\zeta_0 + \zeta_1 - R^2\mu_2)/R^2, \\
 C_{11} &= (R\zeta_1 + \zeta_2)/R^2, \quad C_{12} = (R\eta_1 + \eta_2)/R^2, \\
 C_{21} &= \eta_1/R, \quad C_{22} = \zeta_1/R, \\
 C_{33} &= \zeta_1/R, \quad C_{34} = (R^2\zeta_1 + 2R\zeta_2 + \zeta_3)/R^3, \\
 C_{43} &= \zeta_0 - R\mu_2, \quad C_{44} = (R\zeta_1 + \zeta_2)/R^2, \\
 D_{11} &= -(R\zeta_2 + \zeta_3)/R^3, \quad D_{12} = -\eta_2/R^2, \\
 D_{14} &= \eta_1/R, \quad D_{21} = -\eta_2/R^2, \\
 D_{22} &= -(-R\zeta_0 + \zeta_1 + R^2\mu_1)/R, \quad D_{24} = \zeta_0 - R\mu_1, \\
 D_{33} &= -(2R\zeta_2 + \zeta_3)/R^3, \\
 D_{43} &= -(\zeta_2 - R^2\zeta_0 + R\zeta_1 + R^3\mu_2)/R^2,
 \end{aligned}$$

where

$$\begin{aligned}
 \xi_i &= \int_{-h/2}^{h/2} \frac{E}{1-v^2} z^i dz, \quad \eta_i = \int_{-h/2}^{h/2} \frac{vE}{1-v^2} z^i dz, \\
 \zeta_i &= \int_{-h/2}^{h/2} \frac{E}{2(1+v)} z^i dz, \quad (i = 0, 1, 2, 3), \\
 \mu_1 &= \int_{-h/2}^{h/2} \frac{E}{1-v^2} \frac{dz}{R+z}, \quad \mu_2 = \int_{-h/2}^{h/2} \frac{E}{2(1+v)} \frac{dz}{R+z}.
 \end{aligned}$$

When the thickness of the inner layer equals that of the outer layer ( $t_1 = t_3$ ) then

$$\zeta_1 = \zeta_3 = 0, \quad \eta_1 = \eta_3 = 0, \quad \zeta_1 = \zeta_3 = 0.$$

**Appendix B**

Constants with superscript star in Eqs. (13)–(15) are given by

$$\begin{aligned}
 A_{12}^* &= A_{12} + A_{44}, \quad B_{12}^* = B_{12} + B_{43}, \quad A_{34}^* = A_{34} + C_{34}/R, \\
 A_{22}^* &= A_{22} + C_{22}/R, \\
 A_{21}^* &= A_{21} + A_{33} + (C_{21} + C_{33})/R, \quad B_{22}^* = B_{22} + D_{22}/R, \\
 B_{21}^* &= B_{21} + B_{33} + (D_{21} + D_{33})/R, \quad B_{24}^* = B_{24} + D_{24}/R, \\
 D_{12}^* &= D_{12} + D_{21} + D_{33} + D_{43}, \\
 D_{14}^* &= D_{14} - RB_{21}, \quad D_{24}^* = D_{24} - RB_{22}, \\
 C_{21}^* &= C_{21} + C_{33} + C_{43}, \quad C_{12}^* = C_{12} + C_{34} + C_{44}.
 \end{aligned}$$

**Appendix C**

Expressions for coefficients in Eqs. (19)–(21) are

$$\begin{aligned}
 a_{11} &= \zeta_0^* + m^2 \delta \mu_2^*/\lambda_n^2, \quad a_{12} = -m(\eta_0^* + \zeta_0^*)/\lambda_n, \\
 a_{13} &= -\frac{1}{12\delta^2} \lambda_n \zeta_2^* + (\delta \mu_2^* - \zeta_0^*)m^2/\lambda_n - \eta_0^*/\lambda_n, \\
 a_{21} &= a_{12}, \quad a_{22} = \zeta_0^* + \frac{\zeta_2^*}{4\delta^2} + m^2 \zeta_0^*/\lambda_n^2, \\
 a_{23} &= \frac{3\zeta_2^* + \eta_2^*}{12\delta^2} m + m \zeta_0^*/\lambda_n^2, \quad a_{31} = a_{13}, \quad a_{32} = a_{23}, \\
 a_{33} &= \frac{1}{12\delta^2} \lambda_n^2 \zeta_2^* - m^2 \left( \zeta_0^* - \delta \mu_2^* - \frac{2\eta_2^* + 3\zeta_2^*}{12\delta^2} \right) \\
 &\quad + [(\delta \mu_1^* - \zeta_0^*)(m^4 - 2m^2) + \delta \mu_1^*]/\lambda_n^2,
 \end{aligned}$$

where

$$\begin{aligned}
 \delta &= \frac{R}{h}, \\
 (\zeta_0^*, \eta_0^*, \zeta_0^*) &= (\zeta_0, \eta_0, \zeta_0)/C, \\
 (\zeta_2^*, \eta_2^*, \zeta_2^*) &= (\zeta_2, \eta_2, \zeta_2)/D, \\
 (\mu_1^*, \mu_2^*) &= h(\mu_1, \mu_2)/C,
 \end{aligned}$$

$$D = \frac{E_1 h^3}{12(1-v_1^2)}, \quad C = \frac{hE_1}{1-v_1^2}.$$

For the FG middle layer with its Young’s modulus given by Eq. (5), we have

$$\begin{aligned}
 \zeta_0^* &= 1 - \beta + \phi\beta(k + 1)/2, \\
 \eta_0^* &= (1 - \beta)v_1 + v_2\phi\beta(k + 1)/2, \\
 \zeta_0^* &= (1 - v_1)(1 - \beta)/2 + (1 - v_2)\phi\beta(k + 1)/4, \\
 \zeta_2^* &= 1 - \beta^3 + \phi\beta^3(k + 3)/4, \\
 \eta_2^* &= v_1(1 - \beta^3) + v_2\phi\beta^3(k + 3)/4, \\
 \zeta_2^* &= (1 - v_1)(1 - \beta^3)/2 + (1 - v_2)\phi\beta^3(k + 3)/8,
 \end{aligned}$$

$$\begin{aligned}
 \mu_1^* &= \ln \frac{2\delta + 1}{2\delta - 1} - \ln \frac{2\delta + \beta}{2\delta - \beta} \\
 &\quad + \phi \left[ k \ln \frac{2\delta + \beta}{2\delta - \beta} + 2 \frac{\delta}{\beta} (1 - k) \ln \frac{4\delta^2}{4\delta^2 - \beta^2} \right], \\
 \mu_2^* &= \frac{1 - v_1}{2} \left( \ln \frac{2\delta + 1}{2\delta - 1} - \ln \frac{2\delta + \beta}{2\delta - \beta} \right) + \phi \frac{1 - v_2}{2} \\
 &\quad \times \left[ k \ln \frac{2\delta + \beta}{2\delta - \beta} + 2 \frac{\delta}{\beta} (1 - k) \ln \frac{4\delta^2}{4\delta^2 - \beta^2} \right].
 \end{aligned}$$

When Young’s modulus for the material of the middle layer is given by Eq. (6), we have

$$\zeta_0^* = 1 - \beta + \phi\beta(2k + 1)/3,$$

$$\eta_0^* = (1 - \beta)v_1 + v_2\beta\phi(2k + 1)/3,$$

$$\zeta_0^* = (1 - v_1)(1 - \beta)/2 + (1 - v_2)\phi\beta(2k + 1)/6,$$

$$\zeta_2^* = 1 - \beta^3 + \phi\beta^3(2k + 3)/5,$$

$$\eta_2^* = v_1(1 - \beta^3) + v_2\phi\beta^3(2k + 3)/5,$$

$$\zeta_2^* = (1 - v_1)(1 - \beta^3)/2 + (1 - v_2)\phi\beta^3(2k + 3)/10,$$

$$\mu_1^* = \ln \frac{2\delta + 1}{2\delta - 1} - \ln \frac{2\delta + \beta}{2\delta - \beta} + \phi \left[ k \ln \frac{2\delta + \beta}{2\delta - \beta} + 4(1 - k) \left( \frac{\delta^2}{\beta^2} \ln \frac{2\delta + \beta}{2\delta - \beta} - \frac{\delta}{\beta} \right) \right],$$

$$\mu_2^* = \frac{1 - v_1}{2} \left( \ln \frac{2\delta + 1}{2\delta - 1} - \ln \frac{2\delta + \beta}{2\delta - \beta} \right) + \phi \frac{1 - v_2}{2} \times \left[ k \ln \frac{2\delta + \beta}{2\delta - \beta} + 4(1 - k) \left( \frac{\delta^2}{\beta^2} \ln \frac{2\delta + \beta}{2\delta - \beta} - \frac{\delta}{\beta} \right) \right],$$

where

$$\phi = \frac{1 - v_1^2}{1 - v_2^2}, \quad \beta = \frac{t_2}{h},$$

## References

- [1] Novozhilov VV. Thin shell theory. (Translated by Lowe PG). Groningen, The Netherlands: P Noordhoff Ltd.; 1964.
- [2] Flügge W. Stresses in shells. 2nd ed. New York: Springer-Verlag; 1973.
- [3] Bush BO, Almroth BO. Buckling of bars, plates and shells. New York: McGraw-Hill; 1975.
- [4] Theodore von K, Hsue-Shen T. The buckling of thin cylindrical shells under axial compression. *J Aeronaut Sci* 1941;8(8):303–12.
- [5] Winterstetter TA, Schmidt H. Stability of circular cylindrical shells under combined loading. *J Thin-walled Struct* 2002;40: 893–909.
- [6] Kim SE, Kim CS. Buckling strength of cylindrical shell and tank subjected to axially compressive loads. *J Thin-Walled Struct* 2002; 40:329–53.
- [7] Pinna R, Ronalds BF. Buckling and post-buckling of shells with one end pinned and the other end free. *J Thin-walled Struct* 2002;40: 507–25.
- [8] Ru CQ. Effect of van der Waals force on axial buckling of a double-walled carbon nanotube. *J Appl Phys* 2000;87:7227–31.
- [9] Eslami MR, Javahert R. Buckling of composite cylindrical shells under mechanical and thermal loads. *J Therm Stresses* 1999;22: 527–45.
- [10] Eslami MR, Shahsiah R. Thermal buckling of imperfect cylindrical shells. *J Therm Stresses* 2001;24:71–89.
- [11] Hui-Shen S. Postbuckling analysis of axially-loaded functionally graded cylindrical shells in thermal environments. *Compos Sci Technol* 2002;62:977–87.
- [12] Hui-Shen S. Postbuckling analysis of pressure-loaded functionally graded cylindrical shells in thermal environments. *Eng Struct* 2003;22:977–87.
- [13] Weaver PM. Design of laminated composite cylindrical shells under axial compression. *Compos B* 2000;31:669–79.
- [14] Koiter WT, The stability of elastic equilibrium (in Dutch; Doctoral dissertation in Technical Sciences at the Technische Hooze School, Delft, 1945), English translation by Riks, R., Technical report AFFDL-TR-70-25, AFLD, Wright-Patterson Air Force Base, OH, USA, 1970.
- [15] Thompson JMT, Hunt GW. A general theory of elastic stability. London: Wiley; 1973.
- [16] Sears A, Batra RC. Buckling of multiwalled carbon nanotubes under axial compression. *Phys Rev B* 2006;73:085410.